Extreme-ultraviolet frequency combs from high-order harmonic generation with few-cycle pulse trains

Maria Tudorovskaya[*]

University of Edinburgh, Joseph Black Building, David Brewster Road, Edinburgh, Scotland EH9 3FJ, United Kingdom

Manfred Lein

Institut für Theoretische Physik and Centre for Quantum Engineering and Space-Time Research (QUEST), Leibniz Universität Hannover, Appelstraße 2, 30167 Hannover, Germany

The spectrum of a high-repetition train of laser pulses consists of many equally spaced lines, forming an optical frequency comb which is useful for high-precision spectroscopy. By exposing atoms to a train of strong pulses, frequency combs reaching into the extreme ultraviolet may be produced via high-order harmonic generation. Here, we report a theoretical study of extreme-ultraviolet frequency-comb generation by trains of few-cycle pulses. We analyze the nontrivial comb structure arising from overlapping harmonic orders. The spacings of the comb lines and their dependence on the offset frequency of the incident pulse train are discussed.

I. INTRODUCTION

A frequency comb is an ingenious tool providing a modern and elegant method of laser-based high-precision spectroscopy. The essential idea of a frequency comb is that a train of mode-locked laser pulses implies a spectrum consisting of narrow equidistant peaks in the frequency domain, distributed around the central laser frequency [1,2]. Such a spectral ruler with narrow lines is useful for precise measurement of transition frequencies in atoms and molecules [3–7], for atomic clocks [8,9] or for calibration [10]. Pulses within the train are nearly identical, except that the carrier-envelope phase (CEP) changes from pulse to pulse due to intracavity dispersion. The pulse-to-pulse shift can be stabilized by suitable techniques [11–13]. The time delay between two pulses defines the repetition frequency and thus the spacing between the peaks in the frequency domain. Normally, the repetition frequency is of the order of 10–10^3 MHz. Laser pulses as short as a few femtoseconds have been used to obtain frequency combs with broad bandwidth [14].

Substantial effort is currently being put into producing and applying frequency combs at shorter wavelengths. In the UV range, for example, a comb was created from a frequency tripled Ti:sapphire laser field and used for Doppler cooling of trapped ions [15]. Recently, pulse pairs at 213 nm, generated by up-converting pairs of Ti:sapphire pulses, have been used for high-precision spectroscopy of the energy levels in krypton atoms [16]. In the extreme ultraviolet (XUV) spectral range, it is difficult to achieve narrow peaks and adequate power at the same time. Short pulses of XUV light are typically produced by high-order harmonic generation (HHG) [17]. This process requires the interaction of intense driving pulses with atoms or molecules. In HHG, the oscillating laser field ionizes the target and thereafter drives the electron away and back to the parent ion, whereupon the returning electron recombines with the core. The durations of these trajectories determine the electron return energies and thus the emitted photon energies,

which reach to approximately $3.2\,U_p + I_p$, where U_p is the ponderomotive energy and I_p is the ionization potential [18]. For a multicycle pulse, the periodic nature of the electric field, together with the inversion symmetry of atoms, leads to harmonic peaks at odd orders of the incident laser frequency. Using a train of intense pulses leads to additional periodicity and, consequently, a comb structure within the HHG spectrum. Experimentally, however, it has been a challenge to obtain XUV frequency combs and characterize the emitted radiation [19–21]. Cingöz *et al.* [22] achieved sufficient XUV comb intensities to determine the absolute frequency of an argon transition at 82 nm by direct frequency-comb spectroscopy.

Only very few theoretical studies have been dedicated to XUV frequency combs. Numerical simulations of XUV comb creation from hydrogen atoms were carried out by Carrera *et al.* [23]. They presented the first numerical confirmation that the comb structure is transferred from the incident laser field to the high-order harmonics involving a multiplication of the offset frequency by the harmonic order as anticipated by Gohle *et al.* [19] based on energy conservation. Subsequently, Carrera and Chu [24] employed time-dependent density-functional theory to calculate emission spectra from helium atoms. They showed that, for very intense pulses, substantial ionization can destroy the frequency-comb coherence. Zhao *et al.* [25] used the many-mode Floquet theory involving a non-Hermitian generalized Floquet matrix eigenvalue problem. They showed that by variation of the pulse-to-pulse CEP shift the strength of ionization and high-order harmonic generation can be controlled.

Previous studies of XUV frequency combs were focused on HHG from trains of multicycle pulses, which imply well-separated harmonic orders. In this article, we discuss the results of numerical simulations with few-cycle pulse trains. We focus on the intriguing case where harmonic orders overlap due to the shortness of the driving pulses, leading to a dense XUV comb. We show that even for very short driving pulses, the line spacing remains well defined. Although there have been numerous previous studies of HHG with few-cycle pulses [26] in the past, they have not addressed the case of pulse trains with nonzero offset frequency. When pulse trains were considered,

———————
[*]maria.tudorovskaya@ed.ac.uk

as in the theory by Frolov *et al.* [27], the train was assumed to be periodic and the aim was to take the limit of an isolated short pulse by letting the repetition rate go to zero. To the best of our knowledge, there is no published theory on HHG from few-cycle pulse trains with pulse-to-pulse phase shift. Atomic units are used throughout this article.

II. THEORY AND NUMERICAL METHODS

As we are mainly interested in the qualitative description of XUV combs and in the positions of the comb lines, we use a one-dimensional model atom for the numerical simulations. We solve the time-dependent Schrödinger equation (TDSE) for an electron in a soft-core potential V_0 with the additional presence of an external laser field. Using the dipole approximation and the length gauge, the TDSE determining the wave function $\Psi(x,t)$ reads

$$i\frac{\partial\Psi(x,t)}{\partial t} = \left(-\frac{1}{2}\frac{\partial^2}{\partial x^2} + V_0(x) + E(t)x\right)\Psi(x,t), \quad (1a)$$

$$V_0(x) = -1/\sqrt{x^2 + \xi^2}, \quad (1b)$$

where $E(t)$ is the external electric field. We use $\xi = 1.175$, giving the ground-state energy -0.58 a.u. (corresponding approximately to the ionization potential of argon). The electric field is composed of M pulses, with the field of the mth pulse ($m = 0,1,\ldots,M-1$) given by

$$E_m(t) = E_0\sin(\omega_0 t + \phi_m)f(t - t_m), \quad (2)$$

where ω_0 is the optical field frequency, ϕ_m determines the CEP, and $f(t)$ is a trapezoidal or $\sin^2$-shaped envelope. In all the calculations below, the field intensity (cycle-averaged peak intensity) is 2×10^{14} W/cm^2, corresponding to a peak field strength of $E_0 = 0.0755$ a.u., and the driving field frequency is $\omega_0 = 0.06$ a.u., corresponding to a 759-nm wavelength. The phase changes from pulse to pulse by a constant offset phase, $\delta\phi$, i.e.,

$$\phi_m = \phi_0 + m\,\delta\phi. \quad (3)$$

The offset phase is associated with the offset frequency ω_{off} as

$$\omega_{\text{off}} = \omega_r\frac{\delta\phi}{2\pi} = \frac{\delta\phi}{\tau_r}, \quad (4)$$

where τ_r is the repetition period and ω_r is the repetition frequency. For our proof-of-principle calculations, we choose a repetition rate higher than that in a real experiment. This simplifies the graphical presentation of the results. Let $t_m = m\tau_r$ be the time when the mth pulse begins. We assume without loss of generality that $\phi_0 = 0$. The spectrum has a comb structure with local maxima at frequencies ω_k:

$$\omega_k = \omega_{\text{off}} + k\omega_r, \quad k \in \mathbb{Z}. \quad (5)$$

We use the split-operator method [28] to solve the TDSE numerically on a grid with spatial step size 0.12 a.u. The propagation starts from the ground-state wave function obtained by imaginary-time propagation [29]. The spectrum of the emitted HHG photons can be found from the Fourier transform of the dipole acceleration $a(t) = \ddot{d}(t) = -\frac{d^2}{dt^2}\langle\Psi(t)|x|\Psi(t)\rangle$. In order to obtain this quantity, we compute the dipole acceleration independently for each pulse. Let $a_m(t)$ denote the acceleration

for a single pulse with phase ϕ_m calculated in the interval from 0 to τ_r. For a pulse consisting of N optical cycles from beginning to end, we evaluate the wave function over a propagation length of $N + 2$ cycles of length $T_0 = 2\pi/\omega_0$ to obtain the numerical acceleration $a_m^{\text{TDSE}}(t)$ in this range. The additional two cycles ensure that recollisions taking place just after the end of the pulse are not neglected. We then assume that the dipole acceleration is negligible afterwards until the beginning of the next pulse, i.e.,

$$a_m(t) = \begin{cases} a_m^{\text{TDSE}}(t), & 0 < t \leqslant (N+2)T_0, \\ 0, & (N+2)T_0 < t \leqslant \tau_r. \end{cases} \quad (6)$$

The total dipole acceleration is calculated as the sum over all pulses of the train:

$$a(t) = \sum_{m=0}^{M-1} a_m(t - m\tau_r). \quad (7)$$

By taking the modulus squared of the Fourier transform of $a(t)$, we find the XUV comb spectrum. Naturally, increasing the number M of pulses in the train increases the HHG signal. More precisely, if every pulse produces equal signal strength, the total signal is expected to be proportional to M^2 at frequencies where the signal adds up fully constructively. Therefore, the resulting spectra shown in Sec. III have been renormalized by multiplication with an additional factor $1/M^2$ so that the presented peak maxima are found to be nearly independent of M.

In the remainder of this section, we discuss the properties of XUV combs from HHG, in particular the selection rules and the expected line spacing. For a sufficiently long multicycle driving pulse, the spectrum consists of odd harmonic orders. This means that for any integer ν there is a peak centered at $(2\nu + 1)\omega_0$, which itself is a comb of narrow lines, also referred to as "teeth" in what follows. This corresponds to the absorption of $2\nu + 1$ photons from the incident pulse train so that the tooth positions of the XUV comb are given by the following expression [19,23]:

$$\Omega_q^{2\nu+1} = (2\nu + 1)\omega_{\text{off}} + q\,\omega_r, \quad \nu \in \mathbb{N}, \ q \in \mathbb{Z}. \quad (8)$$

Thus, the HHG frequency comb can be considered as a combination of two combs with the spacings defined by the laser frequency and the repetition rate of the train. Only when the pulse-to-pulse phase shift is absent, i.e., $\omega_{\text{off}} = 0$, the tooth positions from different harmonic orders are all multiples of the same frequency ω_r.

Let us consider the situation that each pulse consists of only a few optical cycles. In HHG from a sufficiently short pulse, different harmonic orders overlap and tend to form a continuum. At the same time, the odd-order selection rule for harmonic orders breaks down since the generation process does not repeat periodically. This is the regime of isolated attosecond-pulse generation [30]. Thus, for HHG from a train of such short pulses, we expect that the comb structures of different orders overlap, i.e., teeth originating from the different harmonic orders, are present in the same spectral range. Here, the term "harmonic order" stands for the number of photons absorbed from the driving field. This needs to be distinguished from the labels of the horizontal axes of the HHG

spectra below, where "harmonic order" merely quantifies the frequency of the XUV radiation, following common usage.

A few interesting properties of the XUV comb can be derived in the case that the repetition frequency is a rational multiple of the offset frequency. This means that the pulse train is periodic in the sense that every pulse is repeated with the exact same wave form after a sufficiently long time interval τ_p, defining the frequency $\omega_p = 2\pi/\tau_p$. If there is an additional symmetry such that the pulse is repeated with inverted sign of the electric field at $\tau_p/2$, one finds the selection rule that the harmonic frequencies must be an odd multiple of ω_p, in analogy to the usual odd-harmonic-order selection rule for HHG from one long pulse. In such a case, it is easy to show that the harmonic frequencies can again be written in the form of Eq. (8). To be explicit, we express $\delta\phi \in (0,\pi]$ as a fraction of π,

$$\delta\phi/\pi = N_1/N_2, \tag{9}$$

with two numbers, $N_1, N_2 \in \mathbb{N}$, that do not share a common divisor except the number 1. For odd N_1, the pulse sequence satisfies the ω_p-odd-multiple rule with $\omega_p = \omega_r/(2N_2)$. Since the harmonic offset frequencies are required to be also integer multiples of the fundamental offset frequency $\omega_{\text{off}} = N_1\omega_r/(2N_2)$, it follows that Eq. (8) must hold with odd orders $2\nu + 1$. Then, according to Eq. (8), the distance between the teeth from two neighboring odd harmonics with harmonic orders $2k + 1$ and $2k + 3$ is

$$\Delta\Omega^{2k+1,2k+3} = 2\omega_{\text{off}} + Z\omega_r = (N_1/N_2 + Z)\,\omega_r, \tag{10}$$

with $Z \in \mathbb{Z}$. Therefore the smallest gap between such peaks is

$$|\Delta\Omega|^{\min} = (N_1/N_2)\,\omega_r, \quad \text{if } \delta\phi < \pi/2, \tag{11a}$$

$$|\Delta\Omega|^{\min} = (1 - N_1/N_2)\,\omega_r, \quad \text{if } \delta\phi \geqslant \pi/2. \tag{11b}$$

If two arbitrary, not necessarily neighboring, odd harmonics overlap, the conclusion can be generalized. In general, the smallest obtained spacing is found as the smallest nonzero value of

$$|\Delta\Omega| = |(Z'N_1/N_2 + Z)\omega_r|, \tag{12}$$

with $Z, Z' \in \mathbb{Z}$. The absolute minimum is reached when Z and Z' are chosen such that $Z'N_1 + ZN_2 = 1$, which is certainly possible since N_1 and N_2 have no common divisor except 1. We conclude that the distance between the closest peaks will be

$$|\Delta\Omega|^{\min} = \omega_r/N_2. \tag{13}$$

Interestingly, the same conclusion is reached for any $\delta\phi$ given by Eq. (9), even if the odd-order selection rule does not hold. Allowing even orders in addition to the odd orders in Eq. (8) introduces a factor of $1/2$ into the first term of Eq. (12). At the same time, the absence of the odd-order selection rule implies that N_1 is an even number. Thus, effectively, we obtain the same smallest spacing ω_r/N_2 as before.

In the case $\delta\phi \in (\pi, 2\pi)$, we write $\delta\phi = \pi + (N_1/N_2)\pi$ and see that the odd-order selection rule holds when $N_1 + N_2$ is odd. Analogously to the derivation above, we arrive again at Eqs. (12) and (13).
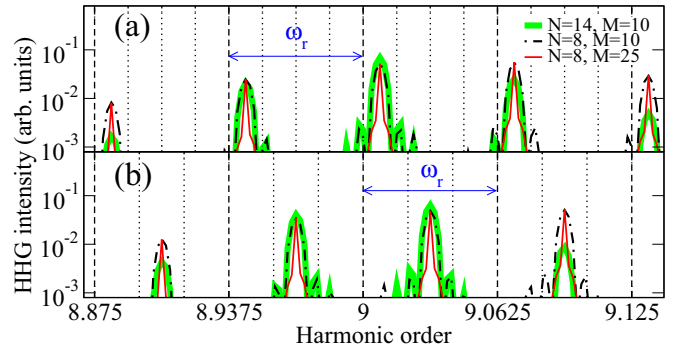

FIG. 1. XUV frequency comb from HHG with multicycle pulses. N denotes the number of optical cycles per pulse. M is the number of pulses in a pulse train. Each pulse has a trapezoidal field envelope with ramps of one optical cycle. The repetition period is $\tau_r = 16T_0$. (a) $\delta\phi = \pi/4$. (b) $\delta\phi = \pi/3$.

III. RESULTS

A. HHG with a train of long pulses

According to Eq. (8), if the pulses in the train are long enough, the teeth within 1 harmonic order are equidistant and separated by ω_r. As an example, Fig. 1 shows calculated HHG spectra around the 9th harmonic from a pulse train with $\tau_r = 16T_0$ and two different carrier-envelope offset phases, $\delta\phi = \pi/4$ or $\delta\phi = \pi/3$. The major grid lines (dashed) are at integer multiples of the repetition frequency $\omega_r = \omega_0/16$. The minor grid lines (dotted) divide the ω_r interval into N_2 segments; see the notation in Eqs. (9) and (13). It is easily verified that the tooth positions follow precisely Eqs. (4) and (8). For the 9th harmonic order, we have $\Omega_q^9 = 9\omega_{\text{off}} + q\omega_r$, $q \in \mathbb{Z}$. For the considered values of $\delta\phi$, this leads to

$$\Omega_q^9 = \begin{cases} \left(\frac{9}{8} + q\right)\omega_r = 9\omega_0 + \left(\frac{1}{8} + q'\right)\omega_r, & \delta\phi = \frac{\pi}{4}, \\ \left(\frac{3}{2} + q\right)\omega_r = 9\omega_0 + \left(\frac{1}{2} + q'\right)\omega_r, & \delta\phi = \frac{\pi}{3}, \end{cases}$$

with $q' \in \mathbb{Z}$. This is in agreement with the numerically found positions.

Comparing different train lengths, one sees that a longer pulse train leads to a better comb with narrow-bandwidth teeth. The shown peak heights are independent of M. Taking into account the renormalization explained in the previous section, this means that the actual signal at the maxima scales as M^2. At the same time, the peaks become narrower with increasing M.

When the number of optical cycles per pulse is increased, harmonic orders become more distinguishable, visible in Fig. 1 (green curve) as a suppression of the comb lines at the low and high end of the shown frequency range.

B. HHG with a train of ultrashort pulses

For HHG from few-cycle pulses, different harmonic orders can overlap in the emission spectrum. This means that XUV combs with different offset frequencies interfere with each other. Nevertheless, if the repetition frequency is a rational multiple of the fundamental offset frequency, the combs are commensurable so that overall a well-defined XUV comb is expected. We demonstrate this behavior by comparing HHG from multicycle pulse trains and few-cycle pulses. Figure 2
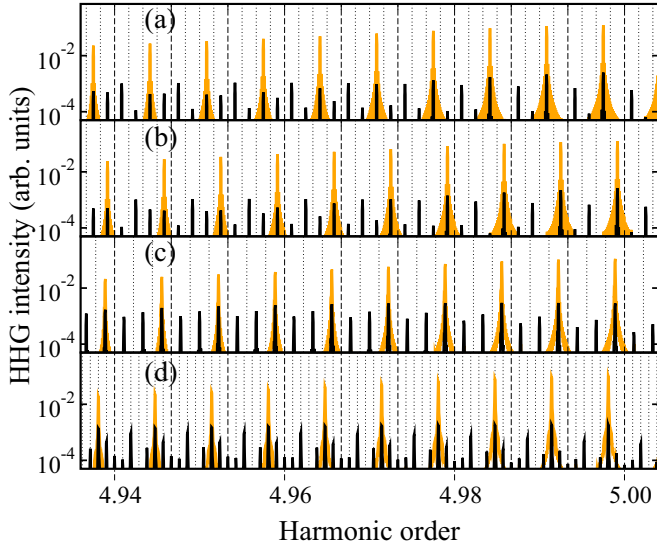
FIG. 2. XUV frequency comb from HHG using trains of 64 long pulses [orange (gray) curves] or 64 short pulses (black curves). The horizontal axis represents an interval around $5\omega_0$. The long pulse has a trapezoidal field envelope of total length $(1 + 46 + 1)T_0$. The short pulse has a $\sin^2$-shaped field envelope of total length $4T_0$. The repetition period is $\tau_r = 150T_0$. (a) $\delta\phi = \pi/4$, (b) $\delta\phi = 3\pi/4$, (c) $\delta\phi = \pi/3$, and (d) $\delta\phi = 2\pi/7$.

shows the emission spectrum near the 5th harmonic order for various $\delta\phi$. Long pulses produce a comb where the teeth are separated by ω_r [orange (gray) curves] and where a five-photon absorption process dominates in the plotted range. The number of photons can be read from the offset of the peaks relative to pure integer multiples of ω_r. In Figs. 2(a) and 2(c), the fundamental offset frequency ω_{off} is one-half of the spacing between the minor grid lines, while in Figs. 2(b) ω_{off} equals

the 1.5-fold grid-line spacing and in Fig. 2(d) ω_{off} is just equal to the grid-line spacing.

The train of few-cycle pulses results in a denser comb (black curves) where the teeth from different harmonic orders (different numbers of absorbed photons) are present. It is not always possible to tell which harmonic order dominates in the region shown.

In all cases shown, the comb spacing in the numerical results is correctly predicted by Eqs. (12) and (13). In Fig. 2(d), for example, the phase shift is $\delta\phi = 2\pi/7$ and the closest peaks are separated by $\omega_r/7$ as follows from Eq. (12) by choosing $Z' = -3$ and $Z = 1$. These results also demonstrate the presence of the odd-order selection rule [Figs. 2(a)–2(c)] or its absence [Fig. 2(d)] depending on the offset frequency.

C. Irrational ratio of offset and repetition frequencies

For long driving pulses, every harmonic order by itself represents a well-defined XUV frequency comb, irrespective of the value of the offset frequency. For very short pulses, the situation is different. In principle, an irrational ratio of offset and repetition frequencies, i.e., $\omega_{\text{off}} = \alpha\omega_r$, $\alpha \in \mathbb{R}\backslash\mathbb{Q}$, leads to an irregular HHG comb. The harmonic frequencies from different numbers of absorbed photons never coincide exactly, although they may contribute to emission in the same region of the spectrum in the case of few-cycle pulses. In this section, we investigate whether a frequency comb structure remains observable and how the transition from long to short pulses proceeds.

In the first example, we consider the phase shift $\delta\phi = \sqrt{2}/2$, giving rise to the offset frequency

$$\omega_{\text{off}} = \sqrt{2}/(4\pi)\,\omega_r \approx 0.11254\,\omega_r. \tag{14}$$

In Fig. 3, we vary the train length for fixed pulse duration to show the development of sharp lines as the number of pulses
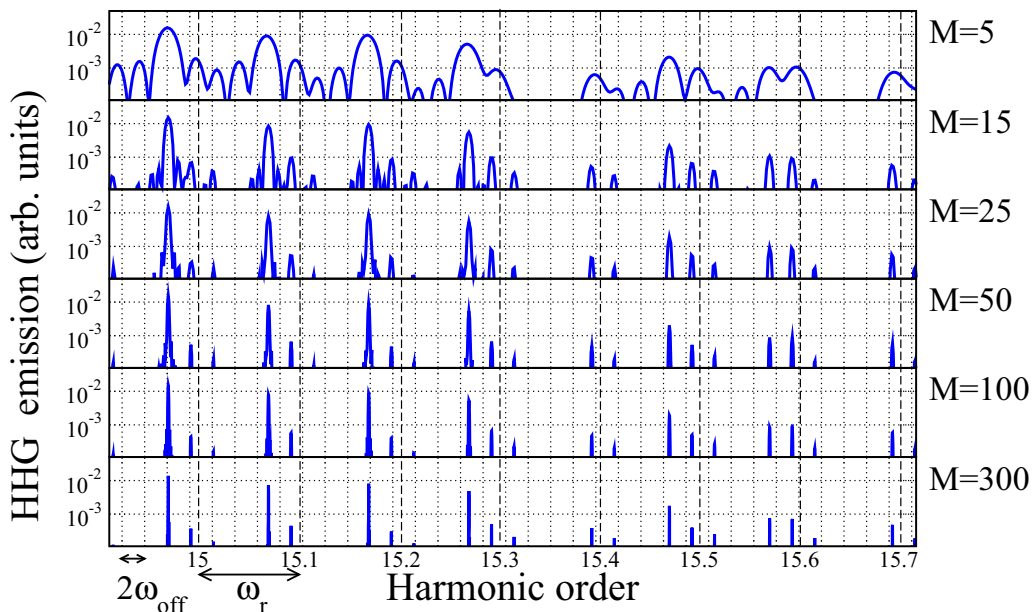

FIG. 3. Structure of the XUV comb depending on the number of pulses, M. The offset phase is $\delta\phi = \sqrt{2}/2$. Each pulse has a trapezoidal field envelope consisting of seven optical pulses, with ramps of length T_0 and a plateau of length $5T_0$. The repetition period is $\tau_r = 10T_0$.
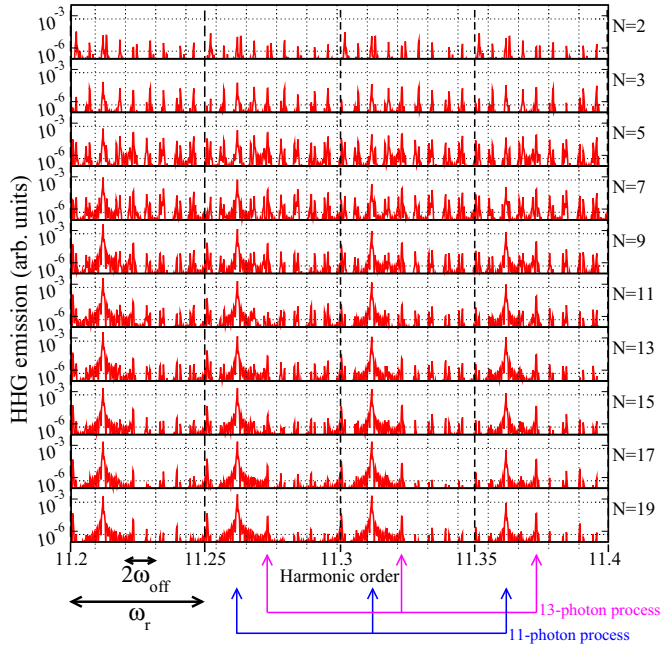
FIG. 4. Structure of the XUV comb depending on the pulse length. N is the total number of optical cycles per pulse. The offset phase is $\delta\phi = \sqrt{2}/2$. The train consists of $M = 200$ pulses. Top panel: $\sin^2$-shaped field envelope; other panels: trapezoidal field envelope with ramps of length T_0. The repetition period is $\tau_r = 20T_0$.

is increased. The HHG spectra around the 15th harmonic from a pulse train consisting of $M \in [5, 300]$ pulses is shown. The major vertical grid lines (dashed) are at frequencies $n\omega_r = 0.1n\omega_0$; the minor vertical grid lines (dotted) divide the axis into segments equal to $2\omega_{off} \approx 0.022\,508\,\omega_0$. The positions of these two grid types' lines never coincide. From the top to the bottom, the train becomes longer. While the peaks are rather broad for a short pulse train ($M = 5$), the teeth become sharper and distinct as M increases. The height of the peak maxima is roughly independent of M, indicating that the actual signal at the peak maxima scales as M^2. However, since the pulse train is not strictly periodic, this scaling is not exact. The dominant teeth, belonging to 15-photon absorption, are separated by ω_r. Next to them, at the distance $2\omega_{off}$, minor teeth attributed to odd harmonics of other orders are visible. They are more than ten times weaker than the main teeth right around $\omega = 15\,\omega_0$, but become of the same order of magnitude as the 15-photon peaks farther on the axis.

Figure 4 shows HHG spectra near the 11th harmonic for another set of calculations. Here, the train duration is kept constant, while the number of optical cycles per pulse, N, increases from the top to the bottom. Due to the significant duration of the train, all the teeth are well distinguishable. In the same manner as above, two types of grid lines are used. The spacing of the dashed grid lines is $\omega_r = 0.05\omega_0$ and the spacing of the dotted grid lines is $2\omega_{off} \approx 0.011\,254\omega_0$. As the pulse becomes longer (from the top to the bottom), the spectrum clears up and it is dominated by the teeth belonging to 11-photon absorption. Secondary teeth are due to the next odd harmonic. The main teeth are separated by ω_r; the minor
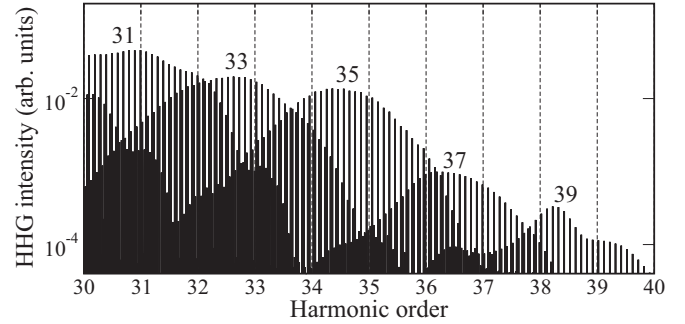

FIG. 5. XUV comb for $\tau_r = 10T_0$, $\delta\phi = 1$, number of pulses $M = 256$, and $\sin^2$-shaped field envelope of seven cycles in total length. The labels $31, \ldots, 39$ indicate the number of absorbed photons from the laser pulse as determined from the offset frequency of the comb lines.

teeth related to 13-photon absorption are separated by $2\omega_{off}$ from the 11-photon peaks.

For very short pulses, there is no obvious distinction into major and minor peaks. Due to the irrational ratio of offset and repetition frequencies, the detailed structure of the spectrum is complicated. Nevertheless, in many cases the spacing between the teeth is about ω_{off}. This can be understood since the number of absorbed photons is limited by the underlying generation process. For example, the maximum number can be estimated using the classical HHG cutoff at $3.2\,U_p + I_p$. Therefore, only a limited range of photon numbers contributes, meaning that the spectrum does not become densely filled with comb lines. Thus, we conclude that it is usually possible to observe an XUV frequency comb.

Different harmonic orders appear as combs with different offset frequencies. The noncommensurability of these combs can be helpful to identify the width of the spectral range associated with each comb, i.e., with a certain photon number. This is illustrated in Fig. 5 where the parameters are chosen as $\tau_r = 10T_0$ and $\delta\phi = 1$. For each comb line, we determine the offset frequency and infer the number of absorbed photons $2\nu + 1$ according to Eq. (8). The different harmonic orders overlap but they become "transparent" due to their comb structure. By visual inspection of the spectrum one can therefore immediately recognize the spectral extension of each number of absorbed photons as indicated in the figure.

IV. CONCLUSION

We have studied theoretically the possibility to generate XUV frequency combs by means of high-order harmonic generation from pulse trains. We have investigated how the structure of the XUV comb depends on the driving laser pulse duration and the train length.

Our study reveals that HHG from few-cycle pulse trains produces overlapping XUV frequency combs corresponding to different numbers of absorbed photons, thus increasing the overall density of the comb. For irrational ratios between offset and repetition frequencies, the harmonics of different orders will never coincide exactly. On the other hand, the order-dependent offset frequency makes the spectrum "transparent" so that the various different photon numbers can be easily identified in the spectrum.

[1] Edited by J. Ye and S. T. Cundiff, *Femtosecond Optical Frequency Comb: Principle, Operation, and Applications* (Springer, New York, 2005).

[2] J. N. Eckstein, A. I. Ferguson, and T. W. Hänsch, High-Resolution Two-Photon Spectroscopy with Picosecond Light Pulses, Phys. Rev. Lett. **40**, 847 (1978).

[3] A. Marian, M. C. Stowe, J. R. Lawall, D. Felinto, and J. Ye, United time-frequency spectroscopy for dynamics and global structure, Science **306**, 2063 (2004).

[4] F. Adler, J. Thorpe, K. C. Cossel, and J. Ye, Cavity-enhanced direct frequency comb spectroscopy: Technology and applications, Annu. Rev. Anal. Chem. **3**, 175 (2010).

[5] J.-D. Deschênes and J. Genest, Frequency-noise removal and on-line calibration for accurate frequency comb interference spectroscopy of acetylene, Appl. Opt. **53**, 731 (2014).

[6] E. Peters, S. Reinhardt, T. W. Hänsch, and T. Udem, Absolute frequency and isotope shift of the magnesium $(3s^2)\,^1S_0 \to (3s3d)\,^1D_2$ two-photon transition by direct frequency-comb spectroscopy, Phys. Rev. A **92**, 063403 (2015).

[7] D. C. Yost, A. Matveev, A. Grinin, E. Peters, L. Maisenbacher, A. Beyer, R. Pohl, N. Kolachevsky, K. Khabarova, T. W. Hänsch, and T. Udem, Spectroscopy of the hydrogen $1s - 3s$ transition with chirped laser pulses, Phys. Rev. A **93**, 042509 (2016).

[8] S. A. Diddams, T. Udem, J. C. Bergquist, E. A. Curtis, R. E. Drullinger, L. Hollberg, W. M. Itano, W. D. Lee, C. W. Oates, K. R. Vogel, and D. J. Wineland, An optical clock based on a single trapped ^{199}Hg$^+$ ion, Science **293**, 825 (2001).

[9] M. Takamoto, F.-L. Hong, R. Higashi, and H. Katori, An optical lattice clock, Nature (London) **435**, 321 (2005).

[10] P. Zou, T. Steinmetz, A. Falkenburger, Y. Wu, L. Fu, M. Mei, and R. Holzwarth, Broadband frequency comb for calibration of astronomical spectrographs, J. Appl. Math. Phys. **4**, 202 (2016).

[11] H. R. Telle, G. Steinmeyer, A. E. Dunlop, J. Stenger, D. H. Sutter, and U. Keller, Carrier-envelope offset phase control: A novel concept for absolute optical frequency measurement and ultrashort pulse generation, Appl. Phys. B **69**, 327 (1999).

[12] A. Apolonski, A. Poppe, G. Tempea, Ch. Spielmann, T. Udem, R. Holzwarth, T. W. Hänsch, and F. Krausz, Controlling the Phase Evolution of Few-Cycle Light Pulses, Phys. Rev. Lett. **85**, 740 (2000).

[13] S. T. Cundiff and J. Ye, Phase stabilization of mode-locked lasers, J. Mod. Opt. **52**, 201 (2005).

[14] S. Rausch, T. Binhammer, A. Harth, F. X. Kärtner, and U. Morgner, Few-cycle femtosecond field synthesizer, Opt. Express **16**, 17410 (2008).

[15] J. Davila-Rodriguez, A. Ozawa, T. W. Hänsch, and T. Udem, Doppler Cooling Trapped Ions with a UV Frequency Comb, Phys. Rev. Lett. **116**, 043002 (2016).

[16] R. K. Altmann, S. Galtier, L. S. Dreissen, and K. S. E. Eikema, High-Precision Ramsey-Comb Spectroscopy at Deep Ultraviolet Wavelengths, Phys. Rev. Lett. **117**, 173201 (2016).

[17] A. McPherson, G. Gibson, H. Jara, U. Johann, T. S. Luk, I. A. McIntyre, K. Boyer, and C. K. Rhodes, Studies of multphoton production of vacuum-ultraviolet radiation in the rare gases, J. Opt. Soc. Am. B **4**, 595 (1987).

[18] P. B. Corkum, Plasma Perspective on Strong Field Multiphoton Ionization, Phys. Rev. Lett. **71**, 1994 (1993).

[19] C. Gohle, T. Udem, M. Herrmann, J. Rauschenberger, R. Holzwarth, H. A. Schuessler, F. Krausz, and T. W. Hänsch, A frequency comb in the extreme ultraviolet, Nature (London) **436**, 234 (2005).

[20] D. Z. Kandula, C. Gohle, T. J. Pinkert, W. Ubachs, and K. S. E. Eikema, Extreme Ultraviolet Frequency Comb Metrology, Phys. Rev. Lett. **105**, 063001 (2010).

[21] I. Pupeza, S. Holzberger, T. Eidam, H. Carstens, D. Esser, J. Weitenberg, P. Rußbüldt, J. Rauschenberger, J. Limpert, T. Udem, A. Tünnermann, T. W. Hänsch, A. Apolonski, F. Krausz, and E. Fill, Compact high-repetition-rate source of coherent 100 eV radiation, Nat. Photon. **7**, 608 (2013).

[22] A. Cingöz, D. C. Yost, T. K. Allison, A. Ruehl, M. E. Fermann, I. Hartl, and J. Ye, Direct frequency comb spectroscopy in the extreme ultraviolet, Nature (London) **482**, 68 (2012).

[23] J. J. Carrera, S.-K. Son, and S.-I. Chu, *Ab initio* theoretical investigation of the frequency comb structure and coherence in the vuv-xuv regimes via high-order harmonic generation, Phys. Rev. A **77**, 031401(R) (2008).

[24] J. J. Carrera and S.-I. Chu, *Ab initio* time-dependent density-functional-theory study of the frequency comb structure, coherence, and dephasing of multielectron systems in the vuv-xuv regimes via high-order harmonic generation, Phys. Rev. A **79**, 063410 (2009).

[25] D. Zhao, F.-l. Li, and S.-I. Chu, Coherent control and giant enhancement of multiphoton ionization and high-order harmonic generation driven by intense frequency-comb laser fields: An *ab initio* theoretical investigation, Phys. Rev. A **87**, 043407 (2013).

[26] T. Brabec and F. Krausz, Intense few-cycle laser fields: Frontiers of nonlinear optics, Rev. Mod. Phys. **72**, 545 (2000).

[27] M. V. Frolov, N. L. Manakov, A. M. Popov, O. V. Tikhonova, E. A. Volkova, A. A. Silaev, N. V. Vvedenskii, and A. F. Starace, Analytic theory of high-order harmonic generation by an intense few-cycle laser pulse, Phys. Rev. A **85**, 033416 (2012).

[28] M. D. Feit, J. A. Fleck, Jr., and A. Steiger, Solution of the Schrödinger equation by a spectral method, J. Comput. Phys. **47**, 412 (1982).

[29] R. Kosloff and H. Tal-Ezer, A direct relaxation method for calculating eigenfunctions and eigenvalues of the Schrödinger equation on a grid, Chem. Phys. Lett. **127**, 223 (1986).

[30] M. Drescher, M. Hentschel, R. Kienberger, G. Tempea, C. Spielmann, G. A. Reider, P. B. Corkum, and F. Krausz, X-ray pulses approaching the attosecond frontier, Science **291**, 1923 (2001).